Università degli Studi di Firenze

DOTTORATO DI RICERCA IN
"Medicina Clinica e Sperimentale"

CICLO XXIV *(Scuola di Medicina Interna Sperimentale Applicata)*

COORDINATORE Prof. Giacomo Laffi

"MR-DWI sequences in the detection of non cystic focal liver lesions: analysis of its clinical role"

Settore Scientifico Disciplinare MED/36

Dottorando
Dott.ssa *Lucarini Silvia*

Tutore
Prof. *Colagrande Stefano*

Anni 2009/2012

Index

Abbreviations:

CA: Contrast agent

FLL: Focal Liver Lesion

MRI: Magnetic Resonance Imaging

DWI: Diffusion-Weighted Imaging

Gd-EOB-DTPA: Gadoxetic Acid

HEM: Haemangioma

FNH: Focal Nodular Hyperplasia

HCC: Hepatocellular Carcinoma

DN: Dysplastic nodule

MTS: Metastases

DYN: Dynamic post-contrast phase

HEP: Hepatobiliary post-contrast phase

1. Preface

Over the past few years tremendous advances in MRI imaging such as the introduction of 3 Tesla magnetic field strength machines, which compared to 0,5T and 1,5 Tesla MRI permit better image quality and a higher signal to noise ratio or such as the introduction of new imaging sequences, in particular spectroscopy, perfusion and diffusion (DWI) imaging, based not anymore on a morphologic study but on a functional study of different tissues.

Spectroscopy imaging analyzes biochemical properties of different tissue and is based on the concept that tissues have different metabolites which present a specific signal that can be measured, since they resonance with known frequencies. For this kind of imaging high field strength machines (1,5-3 Tesla) and specific software are needed.

Perfusion imaging is based on the evaluation of dynamic contrast curves and on the concept that regions with elevated or reduced perfusion can be seen, important in particular in tumor neo-angiogenesis or alterations of the microvasculature in fibrosis and cirrhosis.

Diffusion imaging (DWI), based on the concept of diffusion of water molecules within a tissue, has been first applied to brain studies and it is now being used more frequently in liver, breast, prostate, musculoskeletal, as well as abdominal and pelvic organ imaging. It is increasingly used in liver MRI studies, with promising results for liver lesion detection and characterization.

DW imaging can be easily implemented in clinical protocols, as it can be performed relatively quickly (as short as two breath-hold acquisitions) and does not require contrast agent injection, which makes it attractive in patients with decreased renal function, who cannot receive gadolinium-based contrast agents.

However, DWI of the liver and other abdominal organs is not without its technical challenges.

The liver is a difficult organ to image with magnetic resonance imaging (MRI) because it lies in direct contact with the diaphragm, and the left lobe is inferior to the heart. While good breath-holding technique eliminates the motion of the diaphragm, cardiac motion can cause severe artifacts, especially in the left liver lobe. Bowel peristalsis is another source of motion artifact. Another challenge associated with DWI in the abdomen is the occurrence of susceptibility artifacts resulting from fat and gas interfaces in the abdomen. Modifications

have been made to DWI sequences to help overcome some of the challenges associated with liver imaging.

DWI can be used to compliment the other imaging modalities and it is also showing promise in predicting and monitoring outcome of various treatments for liver cancer such as percutaneous ablative therapy or transarterial catheter chemoembolization.

In literature still some confusion is present regarding especially the acquisition modality of DWI sequences, in particular which b values should be used for a correct study of the liver, and more over for the detection of benign and malignant focal liver lesions.

2. Personal Experience

2.2 *Abstract*

Purpose:

The purpose of this study was to analyze the clinical role of DWI sequences in different FLL, retrospectively comparing it with the other MRI sequences usually performed in a study of the liver for FLL detection.

Materials and Methods:

108 patients (61 male, mean age 59, range 32-81 and 47 female mean age 56.3, range 21-82) who underwent liver MRI for FLL detection were retrospectively analyzed. 307 lesions were detected

(28 haemangiomas, 18 FNH, 42 HCC, 193 MTS, 26 DN).

6 image sets were evaluated: T1+T2 weighted images (T1+T2), diffusion weighted images (DWI), 3D-TFE images in the arterial phase (DYN), hepatobiliary phase Gd-EOB-DTPA -enhanced 3D TFE and FSE images (HEP), combined T1 and T2 weighted images and DW images (T1+T2+DWI) and combined T1 and T2 weighted images and hepatobiliary phase Gd-EOB-DTPA -enhanced 3D TFE and FSE images (T1+T2+HEP). Two observers independently interpreted the images. Detection rate i.e., percentages of detected FLLs was established for each reader and for each image set considering five different groups of lesions by means of primary (Haemangioma, FNH, HCC, DN) or secondary (MTS) nature.

Results:

McNemar test did not show any significant difference among the two observers for each image set.

For HEM the best detection rate is seen with the T1+T2w set (100% for both readers). FNH were best detected with DYN sequences (75% for both readers in FNH< 10mm, 93% for both

readers in FNH > 10mm). Best detection rate for HCC <10mm is reached with the combined set T1+T2+HEP (100% for both readers), for HCC >10mm for reader 1 T1+T2+DWI showed the best detection rate (100%) and for reader 2 T1+T2+HEP set (96%). In MTS DWI sequences showed higher scores than T1+T2w sequences for both readers (P = .000 for both readers) and not statistically significant (P = .064 for both readers) higher rate than HEP set for MTS < 10mm.

For DN T1+T2w set showed statistically significant higher values than DWI set (P = .000 for both readers) with a detection rate of 100% for both readers either for DN <10mm or DN> 10mm.

Conclusions:

In conclusion our study results show that the use of DWI should be considered as a part of liver MR imaging protocols since it has shown equivalent or better detection rate than Gd-EOB-DTPA, especially in MTS with a diameter less than 1cm.

2.3 ***Keywords***

DWI; Gd-EOB-DTPA; FLL

2.4 *Introduction*

DWI imaging has presented as a novelty parameter, which has led to great expectations and disillusions, since initially it was thought to be the solution for the quantitative analysis in detection and characterization (7,9,14,15). of focal liver lesion (FLL), but nowadays many doubts about its real utility raised (16,17).

Therefore after already more than 10 years from its appearance in abdominal MR Imaging it is not yet clear if it contributes in detections of the most common FLL in cirrhotic and non-cirrhotic liver.

DW imaging is based on the concept of the different movement of free versus restricted water molecules; free water is moving according to the Brownian motion, a constant random motion; the water molecules comprised in the cellular microenviroment have many obstacles, such as cellular walls, and therefore a restriction of their diffusion. Since malignant or fibrotic tissue presents a higher cellularity, in these diffusion is much more restricted (1).

DWI has also gained interest because it is a quick sequence (either done in breath hold or free breath acquisition), which can be integrated in the existing protocol either before or after contrast administration; it can be done on virtually every patient, since no contrast material is needed (for example in severe renal dysfunction) (2).

MRI studies of the liver for FLLs detection are mainly based on T1 and T2 weighted unenhanced sequences, followed by sequences acquired after contrast material administration, which became very useful especially with the introduction of hepatospecific contrast agents since in one examination a complete study of the different moments of contrast uptake is now possible, in particular of the dynamic and hepatocyte-specific phases and therefore a better interpretation of lesions characteristics (3,4,5).

In recent years many studies have demonstrated the importance of DWI in detection, characterization of FLLs and in the evaluation of early response after chemotherapy in oncologic patients, and therefore this parameter has been more and more adopted in the state of the art MR liver protocol (6,7).

Giving this background, the purpose of our retrospective study was to evaluate the role of DWI in the detection of non-cystic FLLs, compared with the other sequences adopted in a hepatic MRI study.

2.5 *Material and Methods*

Institutional review board approval and patient consent were not required for this retrospective study because patient privacy was maintained and patient care was not impacted. In fact, patients had provided written informed consent to perform MRI examination with administration of endovenous contrast agent (CA) according to the principles of the Declaration of Helsinki (revision of Edinburgh, 2000). All examinations were performed after overnight fasting.

1. Patients

In our study we retrospectically analyzed 167 patients who underwent an MRI study of the liver at our institution between November 2009 and July 2012 with the administration of gadoxetic acid (Gd-EOB-DTPA) in order to detect, characterize or follow-up focal lesions in non-cirrhotic or cirrhotic liver. The entry criterion for the study choice was the suspicious or known (from patient history and/or other previous exams) presence of a FLL, either benign or malignant (Tab. 1).

Table 1: Patients enrolment flow-chart.

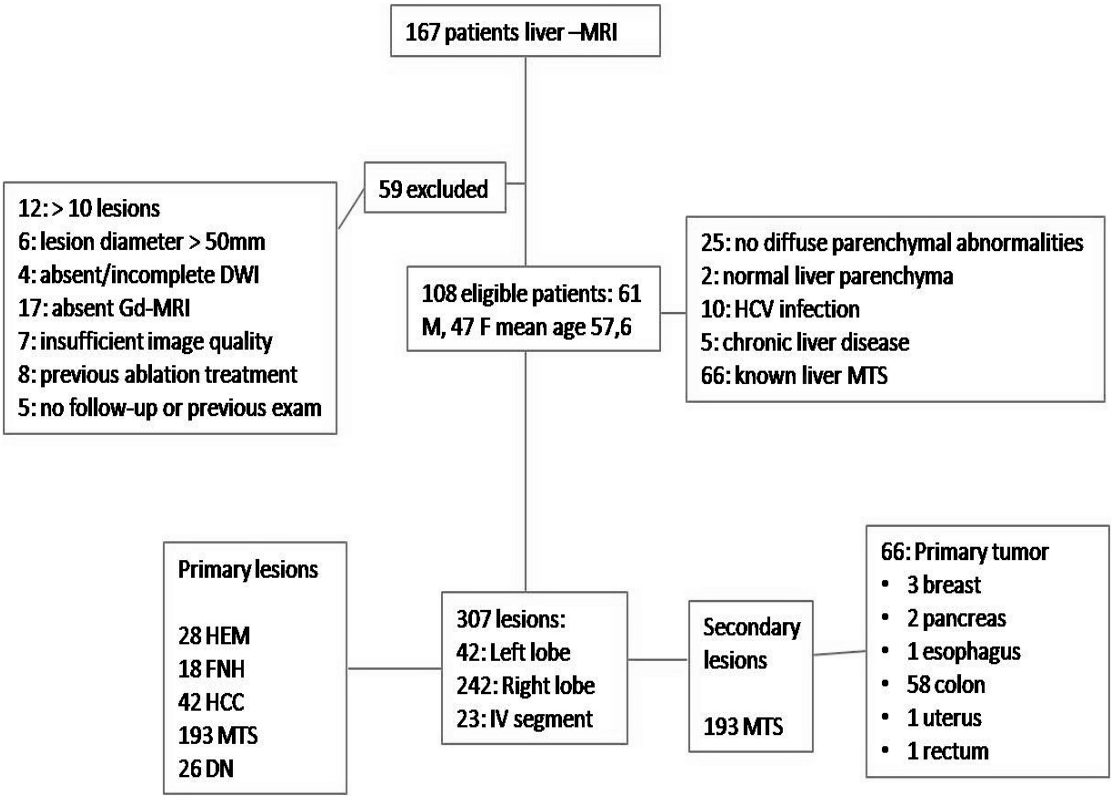

Of this population the following 59 patients were excluded: patients with more than 10 liver lesions (n=12), patients with lesions with maximal diameter > 50mm (n=6), absent or incomplete DW-MRI (n=4), absent Gd-EOB-DTPA-MRI (n=17), insufficient image quality due to respiratory motion artifacts (n=7), previous local ablation treatment (n=8), lack of follow-up or previous examinations (n=5).

Therefore the final study population consisted of 108 patients (61 male, mean age 59, range 32-81 and 47 female mean age 56.3, range 21-82).

Patients with hepatocellular carcinoma (HCC) or Dysplastic nodules (DN) had either normal liver parenchyma (n=2), HCV infection (n=10) or chronic liver disease (n=5).

For patients with metastasis (MTS), primary tumor locations were breast (n=3), pancreas (n=2), esophagus (n=1), colon (n=58), uterus (n=1) and rectum (n=1).

2. *Liver lesions*

In total 307 liver lesions were detected; of these 28 haemangiomas, 18 FNH, 42 HCC, 193 MTS, 26 DN.

The liver has been divided ideally in right lobe (V-V-VII-VIII segment), left lobe (I-II-III) and IV segment: 15 haemangiomas were detected in the right lobe, 11 in the left lobe 2 in the IV hepatic segment. Of FNH 14 were detected in the right lobe, 2 in the left lobe and 2 in the IV segment. Of HCC 33 were detected on the right lobe, 1 in the left lobe and 8 in the IV segment. Of DN 18 were detected in the right lobe, 5 in the left lobe and 3 in the IV segment.

Of MTS 162 were detected in the right lobe, 23 in the left lobe and 8 in the IV segment.

The patient characteristics are summarized in Table 2.

Table 2. Patient population characteristics

Age (mean age)	Male 32-81 years (59 years) Female 21-82 years (56.3 years)
Sex (M/F)	61/47
Diagnosis of the lesions (n=307)	
Benign (n= 72)	28 HEM 18 FNH 26 DN
Malignant (n=235)	42 HCC 193 MTS
Location of the lesion	242 right lobe 42 left lobe 23 IV segment 3 breast
Primary tumor in metastatic patients (n=66)	2 pancreas 1 oesophagus 58 colon 1 uterus 1 rectum

3. *Imaging protocol*

All MR examinations were performed on a 1.5 T MR system (Gyroscan ACSNT Intera Release 12, Philips, Eindhoven, The Netherlands, maximum gradient strength 30 mT/m). A four-element phased-array surface coil (SENSE) was used and positioned to cover the entire upper abdomen in the supine position, with arms extended above the head to reduce blood-flow artifacts.

Patients did not eat for 6 hours prior to the MRI examination.

Before administration of CA we acquired:

- T1-weighted sequence IP-OP (gradient echo-double echo (GEDE), TR =542 msec, TE=15 msec, 395-mm FOV, 256×205 matrix, SENSE factor 1,4, section thickness 6 mm).
- single shot T2-weighted TE80 (sSSh-TE80) sequence (TR=442 msec, TE=80 msec, α=90°, 415-mm FOV, 268x150 matrix, SENSE factor 1,5, section thickness 4 mm) were acquired.

In addition we acquired:

- Breath-hold axial single shot echo planar (EPI) DWI BH b 750 : TR=916 msec; TE=74 msec; b factors 0 and 750 sec/mm²; 128×68 matrix size, 395-mm FOV; section thickness 9 mm; NSA 2; half-scan factor 0.703; acquisition time 18s.
- Axial single shot echo planar (EPI) DWI 16 b short : TR=1800 msec; TE=61 msec; 16 b factors with values from 0 to 750 sec/mm²; 112×64 matrix size, 370-mm FOV; section thickness 9 mm; NSA 3; half-scan factor 0,629; acquisition time 4min 13s; SENSE factor 2.

Then, 25 μmol/kg body weight of gadoxetic acid (then 1 ml per 10 kg weight) was administered at 1 mL/sec intravenously as recommended with a mechanical power injector (Spectris Solaris EP, MedRad, Indianola, PA) through a 20G catheter inserted into an antecubital vein, followed by a 20-mL saline flush at the same injection rate and T1-weighted 3D turbo field echo (T1-TFE) imaging sequences THRIVE (high resolution isotropic voxel examination) were acquired with the following parameters: TR =3,5 msec, TE=1,7 msec, α=10°, 405-mm FOV, 164x114 matrix, SENSE factor 1,5, section thickness 2,5x2,5x2,5

In particular, the sequences were acquired:

- during hepatic artery phase (HAP) with a delay determined by Care Bolus technique (mean delay time, about 30 sec).
- during portal vein phase (PVP) at approximately 75sec.
- during the equilibrium phase at 180 sec.
- during the hepatobiliary phase at 5, 10, 15, and 20 minutes.

The Care Bolus technique in the sagittal and para-sagittal orientations was used to determine the exact time to begin the artery phase acquisition, considering one scan per second. The region of interest (ROI) with appropriate size was located in the abdominal aorta at the level of the celiac trunk. The Care Bolus reached the ROI level after 20–25 s, on the average; we began the THRIVE sequence acquisition by an automatic breath-hold (expiratory) recorded

voice command (given 6 s in advance to the start of the acquisition). Data of imaging protocol are summarized in Tab.3.

Table 3: Imaging protocol characteristics

	T1w sequence IP-OP (gradient echo-double echo (GEDE)	Single shot T2w TE80 (sSSh-TE80)	Breath-hold axial single shot echo planar (EPI) DWI BH b 750	Axial single shot echo planar (EPI) DWI 16 b short	Axial dynamic T1w 3D turbo field echo (T1-TFE) imaging sequences THRIVE
TR/TE (msec)	542/15	442/80	916/74	1800/61	3,5/1,7
Flip Angle (degrees)	80	90	90	90	10
Field of view (mm)	395	415	395	370	405
Matrix	256 x 205	268 x 205	128 x 68	112 x 64	164 x 114
Thickness (mm)	6	4	9	9	2,5 x 2,5 x 2,5
SENSE factor	1,4	1,5	1,5	2	1,5
NSA	1	1	2	3	1
Half-scan factor	(no)	0,69	0,703	0,629	(no)
b-values (s/mm^2)	N/A	N/A	0-750	16 b factors with values from 0 to 750	N/A
Acquisition time	16’	22’	18”	4’ e 13”	18’

4. *Imaging analysis*

Magnetic resonance sequences were divided into 6 image sets:

1. Unenhanced T1 and T2 weighted images (T1+T2).
2. DWI images (DWI)
3. Dynamic Gd-EOB-DTPA -enhanced 3D-TFE images (DYN)
4. Hepatobiliary phase Gd-EOB-DTPA -enhanced 3D TFE and FSE images (HEP)

5. An image set composed by unenhanced T1 and T2 weighted images and DW images (T1+T2+DWI)
6. An images set composed by unenhanced T1 and T2 weighted images and hepatobiliary phase Gd-EOB-DTPA -enhanced 3D TFE and FSE images (T1+T2+HEP).

All image sets were evaluated with a PACS workstation (Infinitt®, Co., Ltd, Seoul, Korea) retrospectively and independently by two radiologists (one with 2 and one with 7 years of experience in abdominal MRI) who were unaware of MRI imaging reports. The image sets were analyzed separately in different sessions with an interval of at least 2 weeks to minimize recall bias. Location and size (maximum axial diameter) were reported for each lesion. When the reviewers expressed discordant opinions, they reached a consensus through a joint review of the recorded images.

The final number of FLL was confirmed by: (1) viewing all sequences together, including therefore T1 and T2 unenhanced sequences, dynamic and hepatobiliary phase Gd-EOB-DTPA-enhanced sequences and DW sequences, (2) previous cross sectional imaging exams, clinical history and pathologic results.

5. *Standard of reference*

The diagnosis of focal liver lesions was proven either by means of needle biopsy (n=27), surgical resection with intraoperative ultrasound within 3 weeks of MRI and histopathological analysis of the resected specimens (n=115) or surveillance by cross sectional imaging (n=165). In this last group of lesions, the standard of reference to distinguish a malignant from a benign lesion was represented by the changing of size (growth or regression) or new occurrence of a lesion compared to previous examinations; in case of HCC the presence of chronic liver disease or elevated serum concentration of alpha-1-fetoprotein was considered; in case of metastases the presence of an underlying primary tumor was considered.

For the characterization of the detected focal liver lesion (FLL) on MRI images the following criteria were applied:

- for Haemangiomas: hypointensity on T1-weighted images and evident hyperintensity on T2-weighted images. On Gd-EOB-DTPA-MRI imaging early peripheral nodular

enhancement with progressive centripetal enhancement on subsequent images (6). On DWI images haemangiomas are hyperintense, mainly because of the T2 shine-trough effect (10).

- For FNH: hypo-isointensity on T1-weighted MR images and iso-hyperintensity on T2-weighted images; hyperintense central scar on T2-weighted images. On Gd-EOB-DTPA-MRI FNH it is hypervascular in the arterial phase and maintains during the hepatospecific phase. (22). On DWI images FNH is generally isointense relative to adjacent liver parenchyma (10).
- For HCC: mostly hypointensity on T1-weighted MR images, generally hyperintensity on T2-weighted images. On Gd-EOB-DTPA-MRI images it shows intense enhancement on the arterial phase, rapid wash-out and presence of a pseudocapsule on the late phase. Variable signal on DWI depending on HCC differentiation (3,10,11).
- For DN: although variable, generally hyperintense on T1-weighted less frequently hypointense and iso- or hypointense on T2-weighted images, without prominent arterial phase enhancement after contrast material administration (11,13).
- For MTS: hypointensity on T1 weighted images, slight hyperintensity on T2 weighted images; hypointensity on arterial, portal-venous, and/or equilibrium phases and/or with perilesional "rim enhancement" in one of the phases; hypointensity and/or with a target appearance in the liver specific phase. More prominent signal intensity on DW Imaging (8,9).

6. *Statistical analysis*

Detection rate i.e., percentages of detected FLLs was established for each reader and for each image set considering five different groups of lesions by means of primary (Haemangioma, FNH, HCC, DN) or secondary (MTS) nature.

McNemar's test was used to identify significant differences in detection rate among all the image sets for each group of FLLs. Moreover, significant interobserver differences in detection rate were identified for each image set using McNemar's test, considering the same groups of FLLs reported above.

To evaluate sensitivity of each image set in detecting FLLs according to their dimension, all analysis were performed including all lesions and separating them by means of maximum diameter (smaller or larger then 10mm).

Statistical analysis was performed using SPSS (version 17.0, SPSS Inc., Chicago). For McNemar's test a p value of 0.05was set as significance threshold.

2.6 *Results*

McNemar test did not show any significant difference among the two observers for each image set. Percentages of detected FLLs are reported in Table 4 and Table 5. Results are summarized in Table 6.

The P value has been mentioned only when statistically significant.

Table 4: Percentages of detected FLLs – results for reader 1.

	Lesion	T1+T2	DWI	DYN	HEP	T1+T2+ HEP	T1+T2+ DWI
< 10 mm	HEM	100% (10/10)	90% (9/10)	80% (8/10)	70% (7/10)	100% (10/10)	100% (10/10)
	FNH	25% (1/4)	50% (2/4)	75% (3/4)	25% (1/4)	50% (2/4)	25% (1/4)
	HCC	67% (10/15)	80% (12/15)	80% (12/15)	87% (13/15)	100% (15/15)	87% (13/15)
	DN	100% (17/17)	29% (5/17)	59% (10/17)	24% (4/17)	100% (17/17)	100% (17/17)
	MTS	77% (71/92)	95% (87/92)		85% (78/92)	90% (83/92)	96% (88/92)
> 10 mm	HEM	100% (18/18)	94% (17/18)	100% (18/18)	100% (18/18)	100% (18/18)	100% 18/18)
	FNH	86% (12/14)	79% (11/14)	93% (13/14)	79% (11/14)	93% (13/14)	93% (13/14)
	HCC	85% (23/27)	93% (25/27)	78% (21/27)	93% (25/27)	96% (26/27)	100% (27/27)
	DN	100% (9/9)	33% (3/9)	89% (8/9)	33% (3/9)	100% (9/9)	100% (9/9)
	MTS	87% (89/102)	99% (101/102)		100% (102/102)	100% (102/102)	99% (101/102)

Table 5: Percentages of detected FLLs – results for reader 2.

	Lesion	T1+T2	DWI	DYN	HEP	T1+T2+ HEP	T1+T2+ DWI
< 10 mm	HEM	100% (10/10)	90% (9/10)	90% (9/10)	70% (7/10)	100% (10/10)	100% (10/10)
	FNH	0% (0/4)	50% (2/4)	75% (3/4)	50% (2/4)	50% (2/4)	25% (1/4)
	HCC	73% (11/15)	80% (12/15)	73% (11/15)	67% (10/15)	100% (15/15)	87% (13/15)
	DN	100% (17/17)	24% (4/17)	71% (12/17)	24% (4/17)	100% (17/17)	100% (17/17)
	MTS	74% (68/92)	92% (85/92)		82% (75/92)	89% (82/92)	94% (86/92)
> 10 mm	HEM	100% (18/18)	89% (16/18)	100% (18/18)	94% (17/18)	100% (18/18)	100% (18/18)
	FNH	79% (11/14)	71% (10/14)	93% (13/14)	71% (10/14)	86% (12/14)	93% (13/14)
	HCC	85% (23/27)	89% (24/27)	81% (22/27)	81% (22/27)	96% (26/27)	93% (25/27)
	DN	100% (9/9)	44% (4/9)	89% (8/9)	33% (3/9)	100% (9/9)	100% (9/9)
	MTS	77% (89/102)	99% (101/102)		95% (97/102)	100% (102/102)	99% (101/102)

Table 6: summarized results comparing the different image sets for each lesion.

Lesion	**Imaging set with best detection rate (%)**
HEM < 10mm	T1+T2w set (100% both readers)
HEM > 10mm	T1+T2w set (100% both readers)
FNH < 10mm	DYN set (75% for both readers)
FNH < 10mm	DYN set (93% for both readers)
HCC < 10mm	T1+T2+HEP set (100% for both readers)
HCC > 10mm	T1+T2+DWI set for reader 1 (100%) T1+T2+HEP set for reader 2 (96%)
MTS < 10mm	T1+T2+DWI set (96% for reader 1, 94% reader 2)
MTS > 10mm	T1+T2+DWI set ≈ T1+T2+HEP set (100% vs 99% for both readers)
DN < 10mm	T1+T2w set (100% for both readers)
DN > 10mm	T1+T2w set (100% for both readers)

1. *Haemangiomas*

For haemangiomas <10mm the best detection rate has been reached already with T1+T2w sequences (100% for both readers) and neither DWI (90% for both readers) nor HEP images (70% for both readers) where useful.

Although also for haemangiomas >10mm T1+T2w set reached 100% of detection rate for both readers with HEP sequences (100% for reader 1 and 94% for reader 2) and DWI (94% for reader 1 and 89% for reader 2) more lesions have been identified when compared with the detection rate of haemangiomas < 10mm.

The combined sets (T1+T2+DWI and T1+T2+HEP) detected 100% of all haemangiomas.

2. *FNH*

FNHs smaller than 10mm were best detected with DYN sequences (75% for both readers); in comparison the T1+T2w set had very low detection rate (25% for reader 1 and 0% for reader 2), DWI had a detection rate of 50% for both readers and HEP images of 25% for reader 1 and 50% for reader 2.

The detection rate of combined sets (T1+T2+DWI and T1+T2+HEP) did not show any differences compared to the DWI and HEP sets (25% for reader 1 and 50% for reader 2).

FNHs with diameter >10mm were best detected with DYN sequences (93% for both readers), but T1+T2w set had better detection rate than in FNH<10mm (86% for reader 1 and 79% for reader 2); DWI and HEP images had the same detection rate (79% for reader 1 and 71% for reader 2). The detection rate of combined sets (T1+T2+DWI and T1+T2+HEP) was better (93% for both for reader 1 and 93% and 86% for reader 2 respectively) than the one of DWI and HEP sets (79% for both for reader 1 and 71% for both for reader 2).

3. *HCC*

For small (<10mm) HCC, then best detection rate is reached with the combined set T1+T2+HEP (100% for both readers). T1+T2 set alone showed a detection rate of 67% for reader 1 and 73% for reader2, HEP set alone a rate of 87% for reader 1 and 67% for reader 2. DWI set alone showed 80% of detection rate and T1+T2+DWI set of 87% for both readers.

In HCC>10mm, for reader 1 T1+T2+DWI showed the best detection rate (100%) and DWI and HEP sets showed the same detection rate (93%). For reader 2 the best detection rate was reached with the T1+T2+HEP set (96% same rate as for reader 1) and DWI set showed higher detection rate than HEP (89% vs 81%).

4. *DN*

With reference to DN < 10mm T1+T2w sequences showed statistically significant higher values than DWI sequences (P = .000 for both readers) with a detection rate of 100% for both readers compared with 29% for reader 1 and 24% for reader 2.

DYN sequences showed statistically significant higher values than the DWI set (P = .008 for reader 1, P = 1.00 for reader 2). HEP set showed low detection rate for both readers (24%).

For DN > 10mm the T1+T2w set showed statistically significant higher values than DWI set (P = .063 for reader 1 and P = .031 for reader 2) with a detection rate of 100% for both readers compared with 33% for reader 1 and 44% for reader 2.

HEP set showed low detection rate for both readers (33%).

The combined sets (T1+T2+DWI and T1+T2+HEP) detected 100% of all DN < and >10mm).

5. *MTS*

When considering secondary lesions (either <10mm or >10mm) DWI sequences showed higher scores than T1+T2w sequences for both readers (P = .000 for both readers) and slightly higher scores than the HEP set for MTS < 10mm, although not with statistical significance (P = .064 for both readers); in fact, the mean percentage of MTS detected by DWI was 95% for reader 1 and 92% for reader 2, whereas the value observed with HEP sequences was 85% and 82% respectively.

When comparing the two last sets, T1+T2+DWI versus T1+T2+HEP no statistically significant differences were found, although the first set showed better detection rate then the second in case of MTS < 10mm (96% vs 90% for reader 1 and 94% vs 89% for reader 2) and a comparable detection rate for MTS>10mm (100% and 99% respectively for both readers).

2.7 *Discussion*

In many cases the correct detection of FLL is of great importance since it often leads the choice of the therapeutic approach; in recent years many studies have compared different imaging sequences, trying to find the best liver MRI imaging protocol. In this study, DWI didn't show significant advantages in the detection of benign FLLs and HCC, but it seems to have a role in detection of MTS, beside Gd-EOB-DTPA-MR imaging.

Taouli et al (23) demonstrated in 2003 that DWI could be a potential supplementary tool in the detection and characterization of FLL, either benign or malignant; since then many authors have analyzed the different MRI sequences, including DWI and post-contrast imaging, but there are limited data on the use of DW imaging for FLL detection (6,21,25,26).

Hussain et al (26) demonstrated that lesion detection is improved in DWI imaging with low b values (20 sec/mm2) optimized by combining parallel imaging, decreased frequency encoding points, and small diffusion gradients. Results of a study by Nasu et al (21) have shown increased detection of metastatic lesions with a combination of DW imaging and precontrast T1- and T2-weighted imaging (82%) compared with pre- and postcontrast (superparamagnetic iron oxide) imaging (66%); Parikh et al (6) demonstrated that detection of malignant and benign FLLs is improved by using DW imaging compared with standard breath-hold T2-weighted imaging and results of another study (27) have demonstrated added detection of tumor foci with DW imaging compared with that with conventional sequences (pre- and postcontrast imaging).

The use of technically better high-resolution 3D gradient-echo (GRE) sequences with fat saturation is well established in recent years not only for early dynamic imaging but also imaging of the hepatocyte phase and it's high performance is demonstrated especially for detecting very small metastases (28).

Shimada et al (15) evaluated the value of DWI and gadoxetic acid-enhanced MR imaging in detection of metastases demonstrating that Gd-EOB-DTPA-enhanced MRI yielded better accuracy in the detection of small hepatic metastases than DWI. Other more recent works, such as the one of Holzapfel et al (7) compared a combination of DWI and gadoxetic acid-enhanced MR imaging and demonstrated that this significantly improved the accuracy and the sensitivity in the detection of FLL, in particular of lesions with a diameter of 10 mm or less.

Our work is different since we have evaluated in non cirrhotic liver all the most frequent benign and malignant FLL separately, with two independent observers, comparing some imaging sets, which analyze sequences considered on their own and in combination (T1+T2w sequences, DWI, DYN, HEP and T1+T2+DWI and T1+T2+HEP); the image sets have been evaluated just for detection of lesions, without considering characterization.

Our results show that DW Imaging doesn't have a significant clinical role in detection of benign FLL, such as haemangiomas and FNH, but this has already been demonstrated (10) and it is known that for the detection of haemangiomas T1 and T2 weighted images are sufficient and for FNH the dynamic phase after contrast administration is diagnostic.

When analyzing malignant lesions the role of DW sequences is different, in particular for HCC. This kind of lesions represents a very heterogenic group, depending on the grade of differentiation of HCC. DW Imaging can be of some utility for the detection of these lesions, although contrast enhanced images in the HEP phase represent the best sequence to detect them; depending on the grading of the HCC this is more or less evident on DWI, and therefore DWI can also help, when the lesion is detected on this sequence, in giving some information about the homogeneity of the lesion itself. This is a proof, on the other hand, that DWI is not sensible to malignant or benign nature but more to homogeneity and inhomogeneity inside the lesion; an example is the well differentiated HCC in Fig 1, not seen on DWI, and the haemangioma on Fig. 2, which is well seen on DWI, because lacunar.

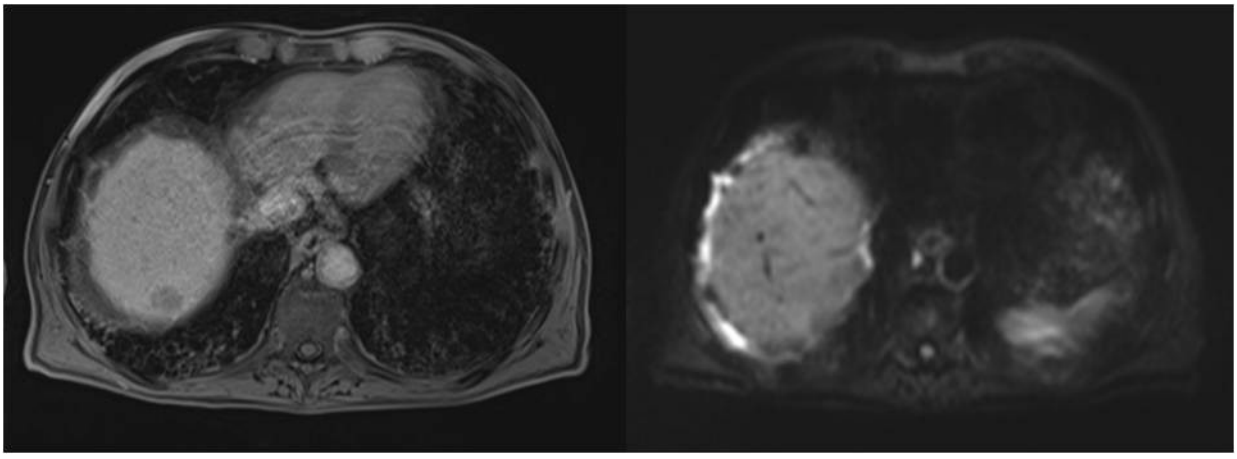

Fig. 1. On the left hepatobiliary phase Gd-EOB-DTPA-enhanced 3DTFE sequence and on the right ss-EPI-DWI sequence in well differentiated HCC; note as this lesion does not appear on DWI images, although it is very evident on the HEP phase.

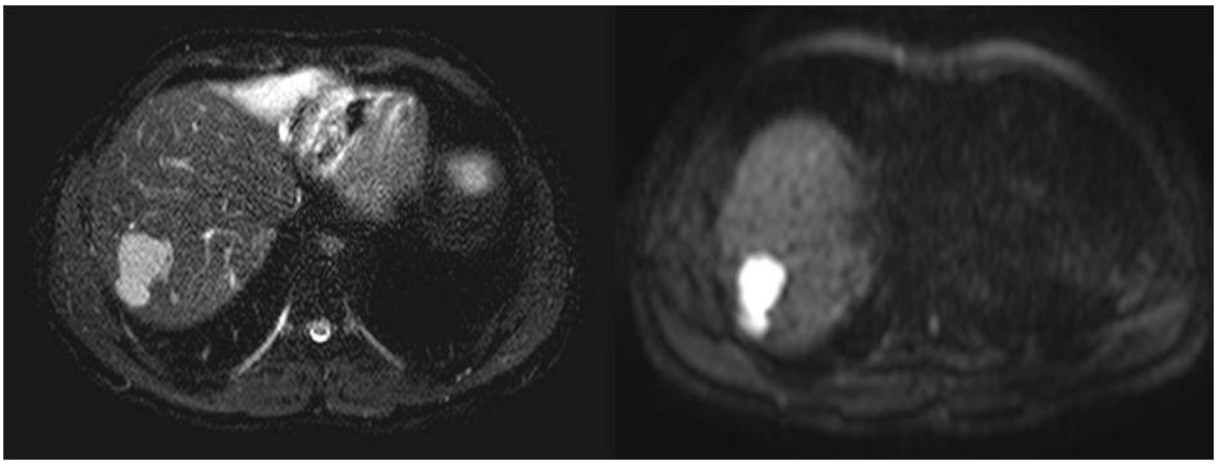

Fig. 2. On the left T2weighted sSSh-TE80 sequence, on the right ss-EPI-DWI sequence in haemangioma. Note the hyper intensity of the lesion on DWI images.

In our study the most important role of DWI is seen in the detection of MTS either with a diameter < 1cm or > 1cm, since it has comparable results to the ones obtained in the hepatospecific phase and therefore it can be suggested as the only additional sequence to T1 and T2 weighted sequences done in the detection of MTS in patients who cannot take contrast material; DWI will then contribute not only to the detection of MTS but also guide their visualization, since it is known (15) that also the smallest MTS appear hyper intense on DWI images, therefore better seen then on the HEP images, in which they are hypo intense; DWI also has the advantage of the black blood effect, which permits a better visualization of metastases lying near vessels, since with small b value (50sec/mm²) a suppression of background vessels, equivalent to that achieved with black-blood images, is obtained with better contrast-to-noise ratio and better lesion conspicuity; this effect represents an advantage compared with contrast enhanced images, in which both lesions and vessels appear hypo intense, and therefore result less visible (32).

The use of low b-values has also the advantage to generate images with a better quality, so even regions which notoriously are difficult to visualize on DWI, such as the left lobe or the hepatic dome, are better seen; this means that DWI could be suggested as a substitute or more an addition to T2 weighted images, as demonstrated by some authors, such as Bruegel et al (30) who compared respiratory-triggered DWI to five different T2-weighted sequences for the

diagnosis of hepatic metastases in 52 patients with 118 lesions at 1.5T and DWI showed higher accuracy (0.91–0.92) compared with T2-weighted fast SE techniques (0.47–0.67). Taouli et al (32) demonstrated that DW images with b values of 50 sec/mm2 had better sensitivity in detection of malignant lesions then standard breath hold T2 weighted images (86.4% versus 62.9%).

Our study has the advantage to compare DWI to the HEP phase on it's own, without considering the rest of the GD-EOB-DTPA phases in the detection of FLL, concluding that especially for metastases with a diameter smaller than 1cm DWI on it's own showed a higher detection rate (95% for reader 1 and 92% for reader 2) then the HEP phase on it's own (85% for reader 1 and 82% for reader 2) and similar conclusions can be done when we compare the combined sets T1+T2+DWI and T1+T2+HEP.

It is also known that on DWI MTS are seen with a greater diameter than the effective one, a phenomenon which is difficult to explain but which could be caused by the fact that the surrounding parenchyma, compressed by the lesion, and therefore more packed, is participating to the signal creation (31).

In the detection of FLL DWI could have a key role when the MRI study is necessary in patients who cannot receive contrast material (because of renal failure, allergies or patients refusal).

Therefore, as the quality of diffusion weighted images is not reduced when DWI is performed after application of the contrast agent, DWI could be added to the liver imaging protocol between the dynamic and the hepatocyte-selective phase without any additional expenditure of time.

In our study we had several limitations. First of all we retrospectively analyzed a large heterogeneous group of lesions, which have not all been proved, but a large number of MTS were confirmed either with histology or on intraoperative ultrasound; some of the benign lesions have been proven histopatologically but for most of them their presence was confirmed by follow-up imaging.

Second, we performed only a qualitative analysis, without measurements of ADC values, lesion enhancement or lesion-liver contrast-to-noise ratio, but this is much more important for lesion characterization than detection.

Moreover, pulse or cardiac triggered DWI may improve liver lesion detection by decreasing artifacts, but it may be difficult to implement and increases the measurement time. Therefore,

we believe that at the state of the art, respiratory- and cardiac-triggered examinations should be employed in a research setting, in attempt to optimize their application.

Our ability to assess false-negative findings was precluded by the fact that our study population did not include patients without FLL.

In conclusion our study results show that DWI helps to improve the detection of FLL, less in case of benign lesions, but in a more significant way in malignant lesions such as MTS and in particular in secondary lesions with a diameter less than 1cm. Therefore, and also because it can be done in the time intercurring between different post-contrast phases, the use of DWI should be considered as a part of liver MR imaging protocols, especially in detection of MTS.

DWI could also be used as the sequence that guides the detection of secondary lesions, since it sometimes represents the only sequences that visualizes them (Fig. 3); this represents an important added value especially in patients who cannot take contrast material.

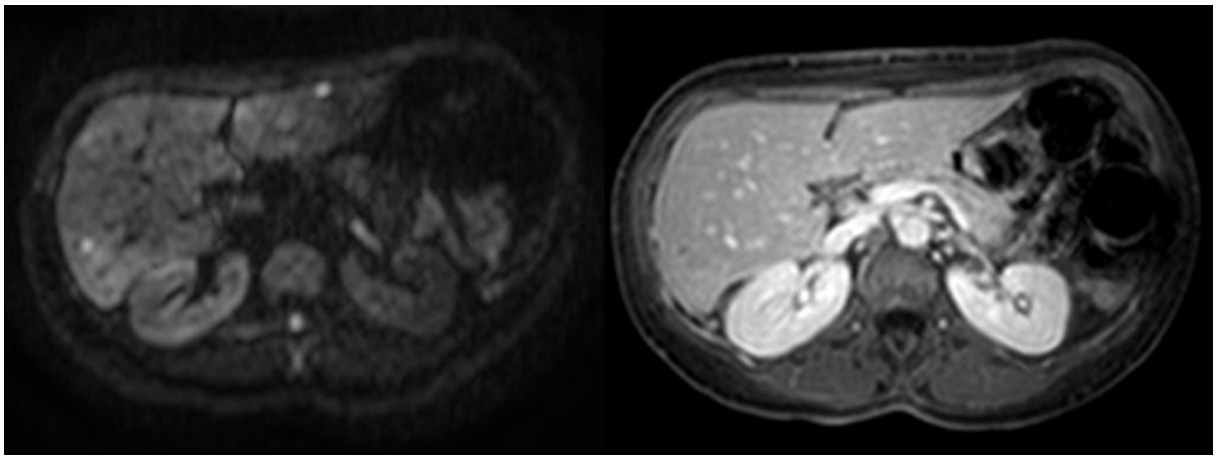

Fig. 3. On the left ss-EPI-DWI sequence and on the right hepatobiliary phase Gd-EOB-DTPA-enhanced 3DTFE sequence in patient with colon metastases; note as the lesion in the VI° segment is slightly evident on the HEP phase image but how the lesion in the II° segment is not detectable on the HEP phase and well evident on DWI images.

Further studies are needed to evaluate the utility of DWI imaging in other applications, such as the assessment of tumor response to treatment and to develop it on new MRI machines, such as 3Tesla MRI.

3. References

1. Malayeri AA, El Khouli RH, Zaheer A, et al. Principles and Applications of Diffusion-weighted Imaging in Cancer Detection, Staging, and Treatment Follow-up. RadioGraphics 2011; 31:1773–1791.
2. Haradome H, Grazioli L, Morone M, et al. T2-weighted and diffusion-weighted MRI for discriminating benign from malignant focal liver lesions: diagnostic abilities of single versus combined interpretations. J MagnReson Imaging 2012 Jun; 35(6):1388-96.
3. Purysko AS, Remer EM, Veniero JC. Focal liver lesion detection and characterization with GD-OEB-DTPA. Clinical Radiology2011; 66:673-684.
4. Grazioli L, Bondioni MP, Haradome H. Hepatocellular adenoma and focal nodular hyperplasia: value of gadoxetic acid-enhanced MR imaging in differential diagnosis. Radiology 2012; 262(2):520-529.
5. Bluemke DA, Sahani D, Amendola M, et al. Efficacy and safety of MR imaging with liver-specific contrast agent: U.S. multi-center phase III study. Radiology 2005; 237:89–98.
6. Parikh T, Drew SJ, Lee VS, et al. Focal Liver Lesion Detection and Characterization with Diffusion-weighted MR Imaging: comparison with Standard Breath hold T2-weighted Imaging. Radiology 2008; 246(3):812-822.
7. Holzapfel K, Eiber MJ, Fingerle AA, et al. Detection, classification, and characterization of focal liver lesions: Value of diffusion-weighted MR imaging, gadoxetic acid-enhanced MR imaging and the combination of both methods. Abdom Imaging 2011; 37:74-82
8. Elsayes KM, Vamsidhar RN, Yuming Y, Govind M, Markus L and Jeffrey JB; Focal Hepatic Lesions: Diagnostic Value of Enhancement Pattern Approach with Contrastenhanced 3D Gradient-Echo MR Imaging.RadioGraphics2005; 25:1299–1320
9. Palmucci S, Mauro LA, Messina M, et al. Diffusion-weighted MRI in a liver protocol: Its role in focal lesion detection. World J Radiol 2012; 4(7):302-310.
10. Silva AC, Evans JM, McCullough AE et al. MR Imaging of Hypervascular Liver Masses: A Review of Current Techniques. RadioGraphics 2009; 29:385-402.

11. Hussain SM, Zondervan PE, Ijzermans JN et al. Benign versus malignant hepatic nodules: MR imaging findings with pathologic correlation. RadioGraphics 2002;22(5): 1023–1036.
12. Purysko AS, Remer EM, Coppa CP. Original Research: Characteristics and Distinguishing Features of Hepatocellular Adenoma and Focal Nodular Hyperplasia on Gadoxetate Disodium–Enhanced MRI. AJR 2012; 198:115-123.
13. Lee MH, Kim SH, Park MJ et al. Original Research: Gadoxetic Acid–Enhanced Hepatobiliary Phase MRI and High-b-Value Diffusion-Weighted Imaging to Distinguish Well-Differentiated Hepatocellular Carcinomas From Benign Nodules in Patients With Chronic Liver Disease. AJR 2011; 197:W868-W875.
14. Coenegrachts K, Delanote J, Ter Beet L et al. Improved focal liver lesion detection: comparison of single shot diffusion weighted echoplanar and single shot T2 weighted turbo spin echo techniques. BJR 2007; 80 (955) 524-531.
15. Shimada K, Isoda H, Hirokawa Y et al. Comparison of gadolinium-EOB-DTPA-enhanced and diffusion-eighted liver MRI for detection of small hepatic metastasis. EurRadiol 2010; 20: 2690-2698.
16. Hardie A, Naik M, Hecht EM et al. Diagnosis of liver metastases: value of diffusion-weighted MRI compared with gadolinium-enhanced MRI. EurRadiol 2010; 20: 1431-1441.
17. Coenegrachts K. Magnetic resonance imaging of the liver: New strategies for evaluating focal liver lesions. WJR 2009; 1 (1):72-85.
18. Kenis C, Deckers F, De Foer B, et al. Diagnosis of liver metastases: Can diffusion-weighted imaging (DWI) be used as a stand alone sequence? European Journal of Radiology 2012; 81:1016-1023
19. Purysko AS, Remer EM, Veniero JC. Focal liver lesion detection and characterization with GD-OEB-DTPA. Clinical Radiology 2011; 66:673-684
20. Choi A, Lee SS, Jung IH, et al. The effect of gadoxetic acid enhancement on lesion detection and characterization using T2weighted imaging and diffusion weighted imaging of the liver. The British Journal of Radiology 2012; 85:29-36
21. Nasu K, Kuroki Y, Nawano S, et al. Hepatic Metastases Diffusion weighted Sensitivity-encoding versus SPIO-enhanced MR Imaging. Radiology 2006; 239 (1):122-130

22. Grazioli L, Bondioni MP, Haradome H. Hepatocellular adenoma and focal nodular hyperplasia: value of gadoxetic acid-enhanced MR imaging in differential diagnosis. Radiology 2012; 262(2):520-529.
23. Taouli B, Vilgrain V, Dumont E, Daire JL, Fan B, Menu Y. Evaluation of liver diffusion isotropy and characterization of focal hepatic lesions with two single-shot echoplanar MR imaging sequences: prospective study in 66 patients. Radiology 2003;226: 71–78.
24. Okada Y, Ohtomo K, Kiryu S, et al. Breath-hold T2-weighted MRI of hepatic tumors: value of echo planar imaging with diffusion-sensitizing gradient. J Comput Assist Tomogr 1998;22:364–371.
25. Moteki T, Sekine T. Echo planar MR imaging of the liver: comparison of images with and without motion probing gradients. J Magn Reson Imaging 2004;19:82–90.
26. Hussain SM, De Becker J, Hop WC, et al. Can a singleshot black-blood T2-weighted spin-echo echo-planar imaging sequence with sensitivity encoding replace the respiratory-triggered turbo spin-echo sequence for the liver? an optimization and feasibility study. J Magn Reson Imaging 2005;21:219–229.
27. Low RN, Gurney J. Diffusion-weighted MRI (DWI) in the oncology patient: value of breathhold DWI compared to unenhanced and gadolinium-enhanced MRI. J Magn Reson Imaging 2007;25:848–858.
28. Zech CJ, Herrmann KA, Reiser MF et al. MR imaging in patients with suspected liver metastases: value of liver-specific contrast agent Gd-EOBDTPA. Magn Reson Med Sci 2007; 6:43–52.
29. Curverwell AD, Sheridan MB, Guthrie JA. Diffusion-weighted MRI of the liver – Interpretative pearls and pitfall. Clin Radiol 2012: 1-9.
30. Breugel Bruegel M , Gaa J , Waldt S , et al . Diagnosis of hepatic metastasis: comparison of respiration- triggered diffusion-weighted echoplanar MRI and five T2-weighted turbo spinecho sequences . AJR Am J Roentgenol 2008 ; 191 : 1421 – 1429.
31. Löwenthal D, Zeile M, Lim WY, et al. Detection and characterization of focal liver lesions in colorectal carcinoma patients: comparison of diffusion-weighted and Gd-EOB-DTPA enhanced imaging. Eur Radiol 2011; 21(4):832-40.
32. Taouli B, Koh DM. Diffusion-weighted MR imaging of the liver. Radiology. 2010; 254(1):47-66.